



Pilot tests of fluid-switcher energy recovery device for seawater reverse osmosis desalination system

Zhaocheng Wang, Yue Wang*, Yanping Zhang, Bingwei Qi, Shichang Xu, Shichang Wang

Chemical Engineering Research Center, School of Chemical Engineering and Technology, Tianjin University, Tianjin 300072, PR China

Tianjin State Key Laboratory of Membrane Science and Desalination technology, Tianjin University, Tianjin 300072, PR China

Tel. +86 22-2740-6889; Fax +86 22-2740-6889; email: tdwy75@tju.edu.cn

Received 1 February 2012; Accepted 30 April 2012

ABSTRACT

Energy recovery devices (ERDs) reduce the power consumption of seawater reverse osmosis (SWRO) systems greatly by recovering the pressure energy in the retentate brine. There are basically two types of ERD in the market, the isobaric type and the centrifugal type. Of which the former achieves rapid progress and holds the leading position in recent years due to its high efficiency. In this article, a pilot-scale fluid-switcher ERD (FS-ERD, isobaric type) was designed and tested under the capacity of 30 m³/h and the operating pressure of 6.0 MPa. The fluid dynamics performances and the efficiency of the device were studied and evaluated. The demonstration shows that the FS-ERD presents good stability with negligible pressure pulsations and high energy recovery efficiency of about 95.9%, which paves the way for the application of FS-ERD in SWRO plants.

Keywords: SWRO; Energy recovery device; Isobaric type; FS-ERD; Pilot tests

1. Introduction

The shortage of freshwater has become an issue of worldwide concern. After years of development, the reverse osmosis technology occupies about 60% of the seawater desalination market and has become an important means of drinking water production [1–3]. Currently, the specific power consumption of seawater reverse osmosis (SWRO) system has been reduced from over 10 kWh/m³ in the 1980s to below 4 kWh/m³ [2], the energy recovery device (ERD) is one of the main contributions and has become an indispensable

consideration in the current SWRO plant design [4], system configuration [5–8] and controlling scheme [9,10] optimization.

There are basically two types of ERD in the market, the centrifugal type and the isobaric type. The centrifugal type transfers the energy via a way of “hydraulic energy to mechanical energy and then to hydraulic energy”, with an efficiency of about 85% in maximum. In contrast, the efficiency of the isobaric type is much higher (above 95%) on account of its direct transferring the hydraulic energy in the retentate brine to the feed seawater [11]. Therefore, the isobaric type has been adopted widely [12–15] and also becomes a research focus broadly [16–19].

*Corresponding author.

In our previous papers published in 2008 [20] and 2010 [21], an innovative isobaric type ERD called fluid-switcher ERD (i.e. FS-ERD) was introduced and investigated. And the focus were on demonstrating the functionality and controlling strategy (stand-alone operation and parallel operation) of the FS-ERD. Nevertheless, the included ERD devices were just principle setups which could not satisfy the real application both in pressure and capacity. Before field test, the device should not only pass the necessary functional tests gratifyingly but also prove itself under industrial conditions.

In this work, an enlarged FS-ERD with a capacity of 30 m³/h was developed and demonstrated in an emulational SWRO system. The main purpose of the tests was to investigate the fluid dynamics performances and energy recovery efficiency of the device under industrial conditions to further improve its design and performance. The present paper describes the results and outcomes of these tests.

2. Description of the FS-ERD

2.1. What is FS-ERD

The FS-ERD is an isobaric type ERD which mainly consists of three components: a rotary fluid-switcher (FS), two pressure cylinders and a check valve nest as shown in Fig. 1. The FS is the core executive part of the FS-ERD, which has four ports and can be considered as an actuated rotary valve essentially. The rotor of the FS gyrates intermittently in the shell driven by a motor. During employment, the high pressure (HP) brine inlet (i.e., Port 1) and low pressure (LP) brine outlet (i.e., port 2) communicate with two cylinders alternately with the rotation of the rotor. The cylinders are the locations for pressure exchanging and fixed with free pistons in each cylinder to prevent the brine and the seawater from mixing. The check valves are used to direct the LP seawater and HP seawater flow in or out of the cylinders respectively.

As an isobaric-type device, the FS-ERD has the same advantages (high efficiency, low noise level, low mixing

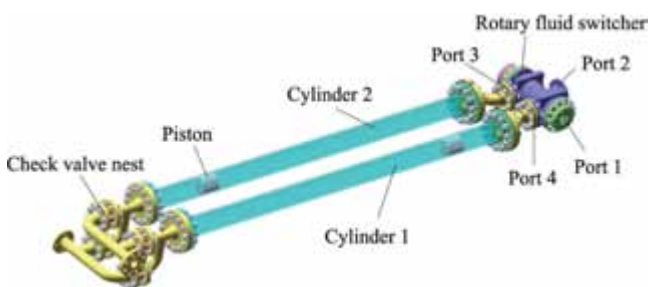


Fig. 1. Basic components of FS-ERD.

percentage, wide operating range, etc.) as commercial products. In addition to these, the internal channels of the FS make it more compact in structure and smaller in size. And the slow operation and electric control provide better accuracy and controllability.

2.2. How FS-ERD works

Fig. 2 shows the configuration of single-stage SWRO process employed with FS-ERD. Therein, the HP brine from the RO membranes passes into the FS-ERD, where its pressure energy is transferred directly to the prefilled LP seawater in one cylinder. The pressurized seawater then passes through a booster pump to compensate its pressure losses and converges with the seawater stream from the HP pump to collectively feed the RO membranes. Simultaneously, the depressurized brine in another cylinder is pumped out by the distributary of the LP seawater feed stream. The sequential alternation of the pressurization and the depressurization strokes in cylinders ensures the continuity of the pressure exchanging and recycling.

2.3. The pilot stand

Referencing to the configuration in Fig. 2, an emulational SWRO system is set up as shown in Fig. 3.

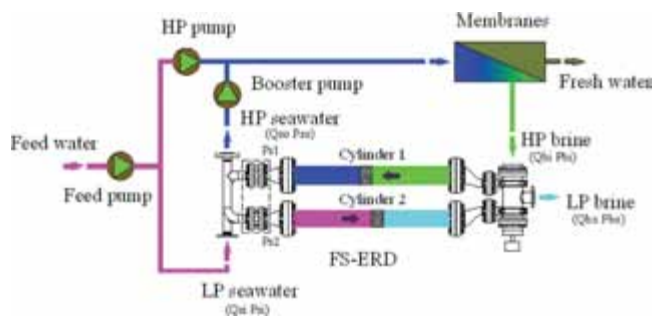


Fig. 2. Configuration of single-stage SWRO system with FS-ERD.

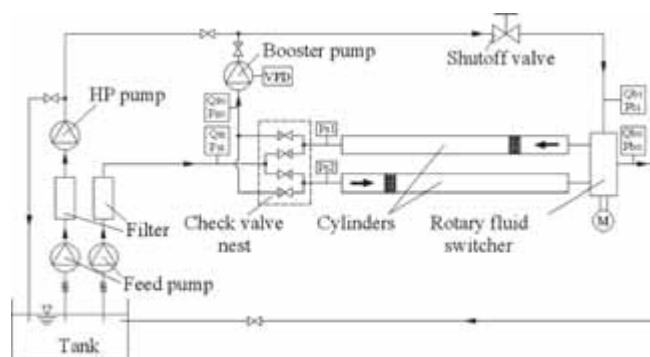


Fig. 3. Flow diagram of the pilot stand.

Wherein, the RO membrane modules are not installed but replaced by a shutoff valve to simulate the flow-through losses of the stream. Tap water is selected as the testing medium for convenience. However, words “seawater” and “brine” are used in this article for easy description. The photograph of the pilot stand is given in Fig. 4.

Programmable logic controller (PLC) system and data-acquisition software are designed and incorporated in the pilot stand. Turbine flow transducers and pressure transducers with a precision of $\pm 0.5\%$ are used to detect the parameters (flow rate and pressure) during the test. All data are collected once per second and can be dynamically displayed on the computer screen through the software, which provides the operator information for monitoring the performance of the FS-ERD instantly.

3. Test results and discussions

3.1. Pressure variations of the cylinder seawater ends

Fig. 5 shows the pressure variations of the cylinder seawater ends Ps1 and Ps2 during the steady-state operation. It indicates that both Ps1 and Ps2 switch between a high level (about 6.0 MPa) and a low level (about 0.3 MPa), just like a rectangular wave. The high level represents the pressurizing stroke, while the low level describes the depressurizing stroke. The two strokes alternate in cylinders when the FS changes its working phase by intermittently rotating the rotor. The short switch time and the two-cylinder design ensure the continuity of the energy recovery.

3.2. Flow rate variations of LP seawater and HP seawater

Fig. 6 shows the flow rate variations of LP seawater (Q_{si}) and HP seawater (Q_{so}) during the steady-state



Fig. 4. Overview of the pilot stand.

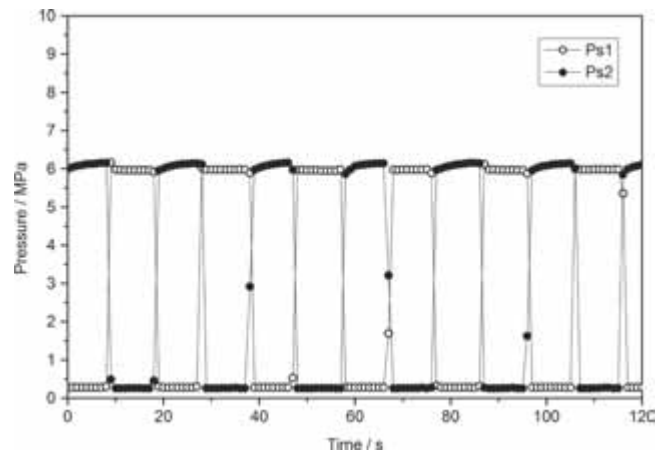


Fig. 5. Pressure variations of the cylinder seawater ends.

operation. It is obvious that Q_{si} and Q_{so} remain constant in most of the time and have the similar regularity. However, visible flow rate downward pulses appeared periodically, which were observed to occur only at the moment of the FS working phase switching. So, it is believed that the causation of the pulses mainly arises from the instant closure between the FS ports and the cylinders, and also the shutting off of the corresponding check valves. The flow rate fluctuations are expected to be reduced or eliminated by means of parallel operation of the FS-ERD [21].

3.3. Pressure variations of seawater streams

Fig. 7 illustrates the pressure variations of LP seawater (P_{si}) and HP seawater (P_{so}) corresponding to the flow rate variations in Fig. 6. It represents that the LP seawater has been pressurized from P_{si} of 0.34 MPa to P_{so} of 6.0 MPa by the FS-ERD. In contrast, the curve of P_{so} is

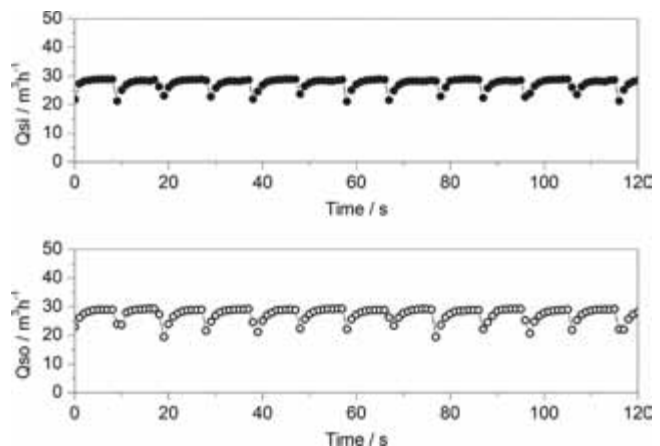


Fig. 6. Flow rate variations of LP seawater and HP seawater with time.

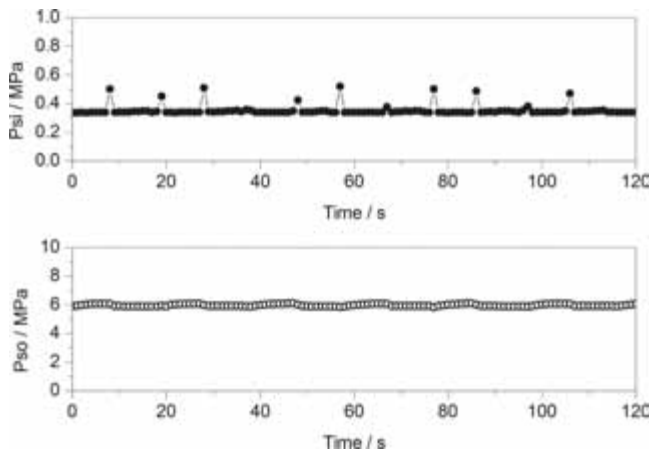


Fig. 7. Pressure variations of seawater streams with time.

more stable than that of Psi, which is necessary and vital for the safety of RO membrane and other equipments. The slight upward pulse of Psi may be caused by the momentary accumulations of stream pressure when the corresponding check valves are closed.

3.4. Pressure variations of brine streams

Fig. 8 shows the pressure variations of HP brine (Pbi) and LP brine (Pbo) during the steady-state operation of FS-ERD. It indicates that the hydraulic energy of the HP brine has been effectively transferred to the seawater and its pressure was reduced from Pbi of 6.0 MPa to Pbo of 0.20 MPa. Here, the Pbi curve remains constant mostly as that of Pso, while Pbo has a periodical downward pulse differently from that of Psi. The downward fluctuations of Pbo are also caused by the switching of the FS and exactly the shrink of LP flow stream. Although pressure fluctuations exist in LP pipelines (Psi and Pbo), their effects on the stability of FS-ERD are negligible.

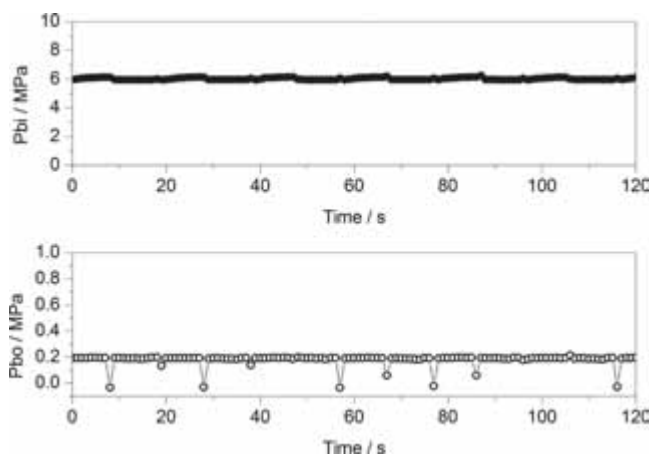


Fig. 8. Pressure variations of brine streams with time.

3.5. Energy recovery efficiency

The energy recovery efficiency of the FS-ERD can be computed according to the following equation:

$$\eta = \frac{\sum \text{Energy}_{\text{out}}}{\sum \text{Energy}_{\text{in}}} = \frac{Q_{so} \cdot P_{so} + Q_{bo} \cdot P_{bo}}{Q_{si} \cdot P_{si} + Q_{bi} \cdot P_{bi}} \quad (1)$$

Based on the steady operating of the FS-ERD, the device's efficiency was assessed and accounts for above 95.9% under the test pressure of 6.0 MPa and capacity of 30 m³/h. The obtained value is not outstanding, but it is comparable with commercial products (91–96%) [17].

4. Conclusions

The main results and outcomes of this work include:

- A pilot-scale FS-ERD was developed and successfully demonstrated in an emulational SWRO system at the operating pressure of 6.0 MPa and capacity of 30 m³/h.
- The fluid dynamics performances indicate that the flow rate and pressure of the influent and effluent streams remain sequentially stable.
- The energy recovery efficiency was assessed and calculated as above 95.9% at the pressure of 6.0 MPa, which stands in the same practical level as the commercial ERDs.

The obtained efficiency and the operating performance indicate that the innovative FS-ERD is reliable and its application in industry is predictable.

Acknowledgements

This research is supported by the National Key Technologies R&D Program (No. 2006 BAB03A021) and the R&D Programs of Tianjin (10JCYBJC04700 and 10ZCKFSH02100).

Symbols

Psi	pressure of the low pressure seawater, MPa
Pso	pressure of the high pressure seawater, MPa
Pbi	pressure of the high pressure brine, MPa
Pbo	pressure of the low pressure brine, MPa
Ps1	pressure of the seawater in cylinder 1 (check valve nest end), MPa
Ps2	pressure of the seawater in cylinder 2 (check valve nest end), MPa

Qsi	flow rate of the low pressure seawater, m ³ /h
Qso	flow rate of the high pressure seawater, m ³ /h
Qbi	flow rate of the high pressure brine, m ³ /h
Qbo	flow rate of the low pressure brine, m ³ /h
η	energy recovery efficiency, %
ΣEnergy _{out}	energy output from the FS-ERD, kW
ΣEnergy _{in}	energy input to the FS-ERD, kW

References

- [1] A.D. Khawaji, I.K. Kutubkhanah and J.-M. Wie, Advances in seawater desalination technologies. *Desalination*, 221 (2008) 47–69.
- [2] M.A. Shannon, P.W. Bohn, M. Elimelech, J.G. Georgiadis, B.J. Marinas and A.M. Mayes, Science and technology for water purification in the coming decades. *Nature*, 452 (2008) 301–310.
- [3] L.F. Greenlee, D.F. Lawler, B.D. Freeman, B. Marrot and P. Moulin, Reverse osmosis desalination: water sources, technology, and today's challenges. *Water Res.*, 43 (2009) 2317–2348.
- [4] V.G. Gude, Energy consumption and recovery in reverse osmosis. *Desal. Water Treat.*, 36 (2011) 239–260.
- [5] A. Zhu, A. Rahardianto, P.D. Christofides and Y. Cohen, Reverse osmosis desalination with high permeability membranes – Cost optimization and research needs. *Desal. Water Treat.*, 15 (2010) 256–266.
- [6] A. Zhu, P.D. Christofides and Y. Cohen, Effect of thermodynamic restriction on energy cost optimization of ro membrane water desalination. *Ind. Eng. Chem. Res.*, 48 (2009) 6010–6021.
- [7] A. Zhu, P.D. Christofides and Y. Cohen, On RO membrane and energy costs and associated incentives for future enhancements of membrane permeability. *J. Membr. Sci.*, 344 (2009) 1–5.
- [8] A. Zhu, P.D. Christofides and Y. Cohen, Minimization of energy consumption for a two-pass membrane desalination: effect of energy recovery, membrane rejection and retentate recycling. *Journal of Membrane Science*, 339 (2009) 126–137.
- [9] A. Ghoheity and A. Mitsos, Optimal time-dependent operation of seawater reverse osmosis. *Desalination*, 263 (2010) 76–88.
- [10] A. Zhu, P.D. Christofides and Y. Cohen, Energy consumption optimization of reverse osmosis membrane water desalination subject to feed salinity fluctuation. *Ind. Eng. Chem. Res.*, 48 (2009) 9581–9589.
- [11] R.L. Stover, Seawater reverse osmosis with isobaric energy recovery devices. *Desalination*, 203 (2007) 168–175.
- [12] B. Schneider, Selection, operation and control of a work exchanger energy recovery system based on the Singapore project. *Desal.*, 184 (2005) 197–210.
- [13] R. Stover and J. Martin, Titan PX-1200 Energy recovery device – test results from the Inima Los Cabos, Mexico, seawater RO facility. *Desal. Water Treat.*, 3 (2009) 179–182.
- [14] R.L. Stover, Retrofits to improve desalination plants. *Desal. Water Treat.*, 13 (2010) 33–41.
- [15] R.L. Stover and J. Martin, Reverse osmosis and osmotic power generation with isobaric energy recovery. *Desal. Water Treat.*, 15 (2010) 267–270.
- [16] W.T. Andrews and D.S. Laker, A twelve-year history of large scale application of work-exchanger energy recovery technology. *Desalination*, 138 (2001) 201–206.
- [17] O.M. Al-Hawaj, The design aspects of rotary work exchanger for SWRO. *Desal. Water Treat.*, 8 (2009) 131–138.
- [18] Y. Zhou, X. Ding, M. Ju and Y. Chang, Numerical simulation on a dynamic mixing process in ducts of a rotary pressure exchanger for SWRO. *Desal. Water Treat.*, 1 (2009) 107–113.
- [19] C.C. Mei, Y.-H. Liu and A.W.-K. Law, Theory of isobaric pressure exchanger for desalination. *Desal. Water Treat.*, 39 (2012) 112–122.
- [20] J. Sun, Y. Wang, S. Xu and S. Wang, Energy recovery device with a fluid switcher for seawater reverse osmosis system. *Chinese J. Chem. Eng.*, 16 (2008) 329–332.
- [21] X. Wang, Y. Wang, J. Wang, S. Xu, Y. Wang and S. Wang, Comparative study on stand-alone and parallel operating schemes of energy recovery device for SWRO system. *Desalination*, 254 (2010) 170–174.